Journal of Operation and Automation in Power Engineering
Vol. 9, No. 3, Dec. 2021, Pages: 203 - 212
http://joape.uma.ac.ir

Optimization of PM Segments Shift Angles for Minimizing the Cogging Torque of YASA-AFPM Machines Using Response Surface Methodology

S.J. Arand *

Electrical Engineering Department, Faculty of Engineering, Yasouj University, Yasouj, Iran

Abstract- *Mitigating the cogging torque is an important issue in designing the YASA machines. The main aim of the paper is to optimize an efficient technique to mitigate the cogging torque of YASA machines. In the suggested technique, the permanent magnets (PMs) are segmented into several segments in the radial direction, and then these PM segments are shifted at appropriate angles in the peripheral direction. The proposed PM segmentation method is compared with the conventional PM segmentation as well as the conventional PM skewing approaches in terms of the amount of cogging torque reduction and the amount of negative impact on the generator load-ability. It is shown that compared to the other two studied approaches, the proposed method is more effective in reducing cogging torque and at the same time, has a less negative impact on the generator output power. Using the suggested technique and via several finite elements based simulations, it is shown that without causing a significant negative impact on the generator load-ability, the generator cogging torque can be reduced considerably (about 90%). By implementing the RSM (Response Surface Methodology), optimal shift angles of the PM segments (factors) are determined to mitigate the cogging torque and maintain the generator load-ability. The experiments are carried out based on the RSM, as an important topic in the statistical DOE (Design of Experiments) approach, to study the impacts of PM segments shift angles on the output power and cogging torque of the YASA-AFPM generator. All of the experimental samples are extracted via the FEA simulations. Also, some of the simulation results are verified using the experimental tests.*

Keyword: AFPM machine, Cogging torque, Magnet segmentation, Multi-objective design, RSM.

1. INTRODUCTION

Axial-flux permanent magnet (AFPM) machines have the exclusive specifications, including compactness, short axial length, high efficiency, and high torque density, which make them appropriate for use in various applications such as traction, wind turbines, and propulsion systems for ships and aircraft [1], [2], [3], [4]. There are various topologies for AFPM machines, including single-sided, double-sided, and multi-sided.

The AFPM topology with a yokeless and segmented armature (YASA) can be considered as state of the art and a specific type of double-sided topology with two outer disk rotors and one internal slotted stator. The YASA topology is relying upon several magnetically separated pieces that create the stator of the YASA-AFPM machine. The torque density of the YASA topology can be increased up to 20% compared to the other AFPM topologies [5]. Also, lack of the stator yoke reduces the iron mass, and thereby reduces the iron losses and improves the YASA-AFPM machine efficiency [6].

The possibility of using the concentrated windings for the YASA topology leads to several advantages such as high-power density and efficiency as well as a simple structure. It is also shown in Ref. [7] that using the concentrated coils in the machine reduces its size and copper losses. Furthermore, in comparison with the distributed winding, due to the non-overlapping feature of the concentrated winding, the coils are physically and thermally separated in a better way, resulting in a reduced phase-to-phase short circuit risk during insulation damage [8].

The cogging torque and eddy current losses in the PMs are some of the issues that could be happened for the surface mounted PMSMs with concentrated coils. The low-order harmonics of the magneto-motive force (MMF) can lead to significant losses in the PMs [9]. Also, for an AFPM wind generator with concentrated windings, these harmonics decrease the expected life of the battery and wind energy converter. Besides, these MMF harmonics may result in outcomes, including

Received: 24 Aug. 2020
Revised: 20 Nov. 2020
Accepted: 16 Jan. 2021
*Corresponding author:
E-mail: s.jamali@yu.ac.ir (S. Jamali Arand)
DOI: 10.22098/joape.2021.7648.1542
Research Paper

copper losses, vibration, noise, and eddy current losses in PMs [10]. To decrease these losses, if they are high, PMs can be partitioned into smaller pieces [11].

Cogging torque as one of the most important subjects in designing the PM machines is caused due to the tendency of PMs to align with the minimum reluctance path [12]. Cogging torque has no net value but has unfavourable impacts on the PM machine performance. The cogging torque component not only affects the self-starting ability of the PM motors but also leads to noise and mechanical vibrations [13]. For a PM wind generator, a high amount of cogging torque can originate problems during the starting of the wind turbine. During start-up, the presence of a high amount of cogging torque can keep the wind turbine at the stall mode [14].

According to the above-mentioned issues, mitigating the cogging torque should be considered at the design stage of PM machines. Several approaches such as using asymmetrical magnets [15], using dual-skew magnets [16], shifting the elementary-cogging-unit [17], using a suitable poles/slots combination [18], using combined rectangle-shaped PMs [19], changing pole arc [20], using round PMs, and applying conventional, triangular, trapezoidal, parallel and double PM skewing [21], and applying variable step skewing [22] have been suggested to minimize cogging torque in the AFPM machines. In Reference [19], ten rectangle-shaped PMs are used at each pole to reduce the cogging torque, and after optimizing the structure, a reduction of about 75% is created in the cogging torque, but at the same time a reduction of about 3.8% is created in the average torque. This method is complicated and difficult for implementing due to the use of 10 pieces of PMs at each pole. Also, in Reference [23], the shaping of the rotor teeth has only led to a 26% reduction in cogging torque but has also led to a 9% increase in the weight of teeth. In Reference [24], a combination of methods such as skewing of PMs, changing the pole arch ratio and the stator shoe width ratio, and shifting the stator shoes has been used to reduce cogging torque, which has led to a complex structure for the motor. In Reference [25], the double-layer PMs are used at each pole to reduce the cogging torque, and after optimizing the structure, a reduction of about 79% is created in the cogging torque, but at the same time a reduction of about 11% is created in the average torque. Due to the structural complexity of the double-layer PMs, this method is difficult to implement.

Most of the above-mentioned techniques suffer from the drawbacks, such as increased cost and complexity and significant adverse impacts on the machine output power. Therefore, an effective technique for mitigating cogging torque in YASA-AFPM generators is suggested, which is based on the fragmenting PMs in the radial direction and shifting some of the segments with suitable shift angles in the circumferential direction. By executing the suggested technique, the cogging torque of the YASA-AFPM machine can be mitigated substantially. Besides, the suggested method would result in lower eddy losses in PMs (due to the magnet segmentation [26]) and negligible adverse impact on the generator load-ability. In this paper, the reference YASA-AFPM machine is presented in Section 2. Then, the cogging torque concept is defined in Section 3. In the next section, the effectiveness of the studied approaches (the proposed PM segmentation, the conventional PM segmentation, and the conventional PM skewing) in reducing the generator cogging torque is investigated via several 3D FEA simulations. In addition, the impact of the studied cogging mitigation techniques on the generator load-ability is investigated in this section. The optimal shift angles of the PM segments (factors) are determined via the RSM approach in Section 5. Finally, conclusions are presented in Section 6.

Table 1. Main parameters of studied YASA-AFPM machine [27]

Parameter	Value	Parameter	Value
Rated power (w)	1000	Rated current (A)	8
Outer diameter (m)	0.18	Pole arc ratio	0.68
Ratio of diameters	0.486	Central bar thickness (m)	0.03
Air-gap length (m)	0.001	Number of segments	12
PM type	N35	Segment shoe thickness (m)	0.005
PM thickness (m)	0.005	Rotor thickness (m)	0.0065
Number of pole pairs	7	Slots/pole/phase	2/7

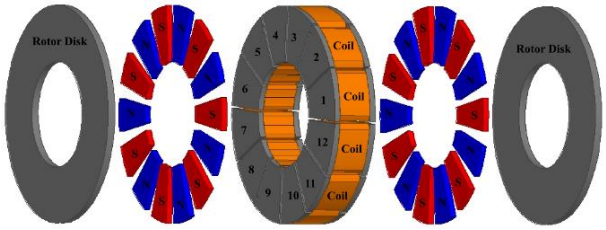

Fig.1. Exploded perspective of investigated YASA-AFPM machine

2. THE REFERENCE YASA-AFPM GENERATOR TOPOLOGY

To evaluate the effectiveness of the suggested cogging torque mitigation technique, a 1 kW YASA-AFPM generator is considered for the study [27]. The main design parameters of the reference studied YASA-

AFPM generator are summarized in Table 1. Figure 1 shows the exploded view of the studied YASA-AFPM machine consisting of 12 segments. A concentrated coil is wounded around each of the segments. The machine consists of two outer disc rotors, and the segmented stator is located between them.

3. COGGING TORQUE IN THE PM MACHINES

According to Eq. (1), cogging torque is a phenomenon resulting from the interaction between the magnetic flux of the PMs located on the rotor surface and the stator reluctance changes arising from the slotting [28].

$$T_{\text{cogg}}\left(\theta_r\right) = -\frac{1}{2}\varphi_{\text{ag}}^2 \frac{d\mathcal{R}}{d\theta_r} \tag{1}$$

Where θ_r is the position of rotor, $\mathcal{R}$ is the reluctance of air-gap, and φ_{ag} is the flux of air-gap. The period of T_{cogg} is:

$$T_{\text{C}} = 360^o / N_c \tag{2}$$

Where N_c is the LCM (least common multiple) of the stator segments and PM poles.

Since there is no specific analytical technique for estimating the cogging torque of a YASA machine, the 3D FEA, as a more accurate technique, is applied to estimate the cogging torque. The 3D FEA provides an appropriate tool for estimating the cogging torque for various machine configurations [21]. The machine air-gap reluctance changes periodically, thus causing the cogging torque to vary as a periodic function [29]. Due to this periodicity, regardless of whether the cogging torque waveform is determined analytically or using the FEA, it can be described by a Fourier series as follows [25]:

$$T_{\text{cog}}\left(\theta_r\right) = \sum_{k=1}^{\infty} T_k \sin\left(kN_c\theta_m + \varphi_k\right) \tag{3}$$

Where T_k and φ_k are the amplitude and phase of the kth harmonic component, respectively.

Although there is no analytical technique to estimate the cogging torque of the AFPM machine, the 3D FEA approach and quasi-3D models can be applied for this aim. Estimating the cogging torque via the quasi-3D technique is faster but less accurate than the 3D FEA. The inherent three-dimensional structure of axial flux machines requires the 3D FEA approach [30], [31]. Due to the symmetry of the machine, only half of the investigated YASA-AFPM generator is modeled. The three-dimensional finite element analysis of the investigated YASA-AFPM generator is done with the help of the Maxwell 16 software package. Since the meshing procedure greatly affects the accuracy of 3D FEA results, to gain more precise results, a finer meshing is used here, especially in the air-gap region; however, this comes at the cost of increased computational time. Numerous studies have indicated that the cogging waveforms estimated via 3D FEA align with those obtained via the experimental tests in terms of amplitude, periodicity, and shape [15], [32], [23], which proves the suitability of the 3D FEA technique for evaluating the cogging torque of AFPM machines. In this paper, to achieve more accurate results, 3D FEA is used to estimate the generator cogging torque.

4. COGGING TORQUE MITIGATION TECHNIQUES

In this section, the conventional PM skewing, the conventional PM segmentation, and the proposed PM segmentation approaches are studied and compared in terms of their effectiveness in reducing the generator cogging torque and their negative impact on the generator output power. The 3D models of the studied generator for the above-mentioned techniques are given in Figure 2. To make the arrangement of PMs perfectly clear, one of the rotor discs is shown transparently. For the PM segmentation methods, S is the number of PM segments.

4.1. Conventional PM skewing approach

The YASA-AFPM machine with skewed PMs is illustrated in Figure 2.b. In the conventional PM skewing method, the most reduction in the cogging torque is provided for a skewing angle equal to the slot pitch angle. The investigated YASA machine has 12 slots and thus its slot pitch angle is 30 degrees. For the YASA machine model with 30 degrees skewed PMs, there is a reduction of about 87% in the cogging torque compared to the original model. The cogging torque waveforms of the original model and the model with skewed PMs are compared in Figure 3.

4.2. Conventional PM segmentation approach

In the conventional segmentation method, the PMs are divided into 2 or 3 segments in the circumferential direction, and some of the segments are shifted with an appropriate shifting angle. The arrangement of the rotor disk and PMs with S = 2 and S = 3 are shown in Figures 4.a and 4.b, respectively. For the S = 2, one PM segment is kept fixed and the other segment is shifted counter-clockwise with the β shift angle. For S = 3, the middle PM segment is kept fixed, one of the other two PM segments is shifted clockwise with the α shift angle, and the remaining PM segment is shifted counter-clockwise with the β shift angle.

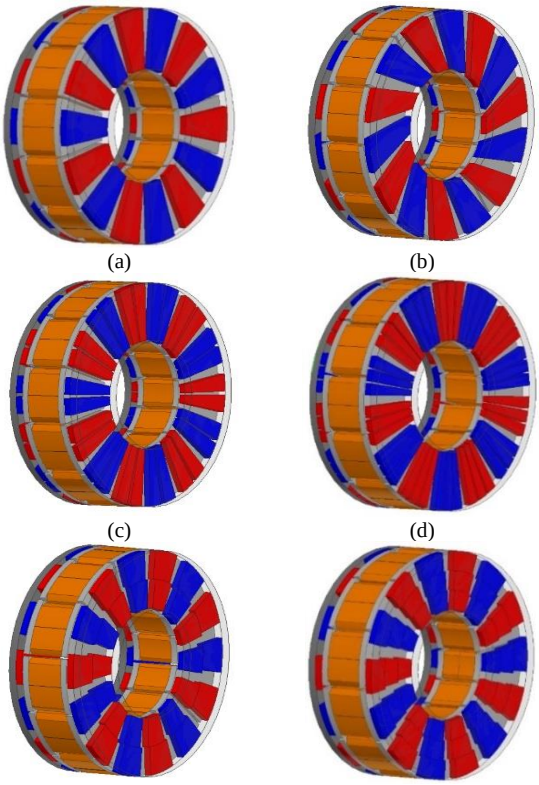

Fig. 2. The 3D models of the YASA generator, (a) Original model, (b) For skewed PMs, (c) For PMs segmented in the circumferential direction (Conventional PM segmentation, S = 2), (d) Conventional PM segmentation, S = 3), (e) For PMs segmented in the radial direction (Proposed PM segmentation, S = 2), (f) Proposed PM segmentation, S = 3

For S = 2 and S = 3, the cogging torque waveforms obtained for some of the studied shifting angles are given in Figures 4.c and 4.d, respectively. As can be seen, for some shifting angles, cogging torque not only does not decrease but also increases. For S = 2, the largest reduction in cogging torque occurs for $\beta = 2^{\circ}$, representing a decrease of approximately 49% compared to the original model. Also, for S = 3, the largest decrease in cogging torque occurs for $\alpha = \beta = 1.25^{\circ}$, representing a decrease of about 39% compared to the original model.

4.3. The proposed PM segmentation approach

The proposed technique is applicable and effective for mitigating the cogging torque in the YASA machines and is based on the segmenting of PMs into 2 or 3 segments in the radial direction and shifting some of these segments in the circumferential direction with suitable shift angles. It is requisite to declare that the PM segments are of equal length in the radial direction.

4.3.1. Magnet segmentation into two segments (S=2)

The arrangement of the rotor disk and PMs are illustrated in Figure 5.a. Each of the PMs is partitioned into 2 segments (S=2). The radial length of the segments is equal. The down segment is held fixed, while the up segment is shifted counter-clockwise with the β shift angle. As shown in Figure 5.b, using several 3D FEA simulations, the cogging torque waveforms are obtained for different shift angles from $\beta = 0^{\circ}$ (Reference machine or Original model) to $\beta = 4^{\circ}$. As can be seen, this approach is very effective in cogging torque mitigation. The lowest peak-to-peak value of the cogging torque is obtained about 0.1395 N.m (approximately 74% reduction comparing the reference machine) and happened for $\beta = 2^{\circ}$. The cogging torque of the reference machine has a peak-to-peak value of 0.536 N.m.

4.3.2. Magnet segmentation into 3 segments (S=3)

The arrangement of the rotor disk and PMs are illustrated in Figure 6.a. Each of the PMs is partitioned into 3 segments (S=3).

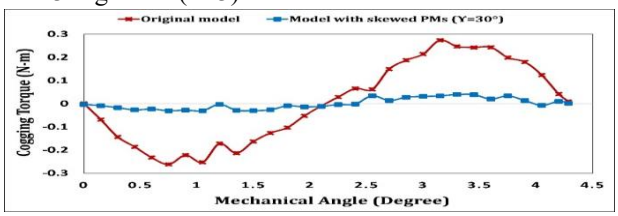

Fig. 3. Comparison of cogging torque waveforms obtained for the original model and model with the skewed PMs

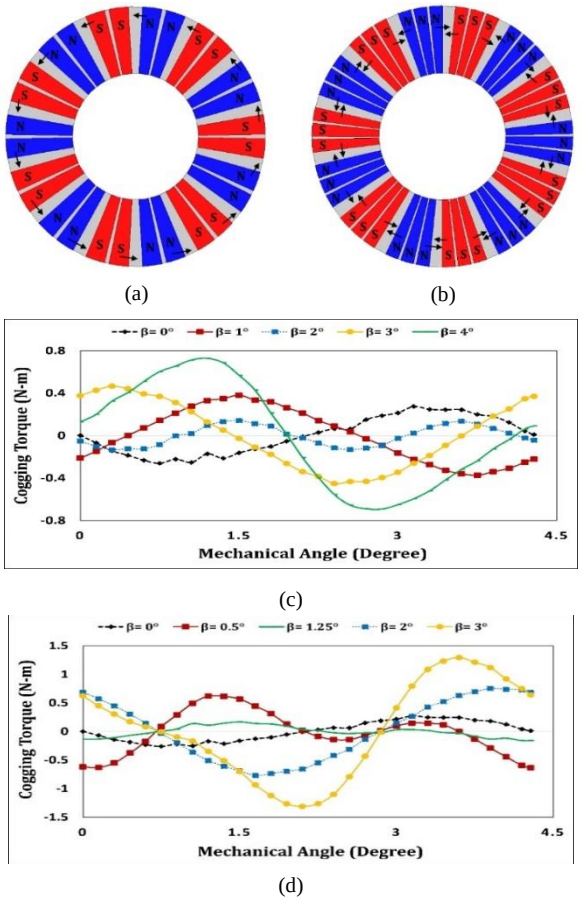

Fig. 4. Conventional PM segmentation, (a) Arrangement of the rotor and PM segments (S=2), (b) Arrangement of the rotor and PM segments (S=3), (c) Cogging torque waveforms for S=2, (d) Cogging torque waveforms for S=3

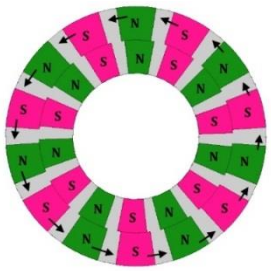

(a)

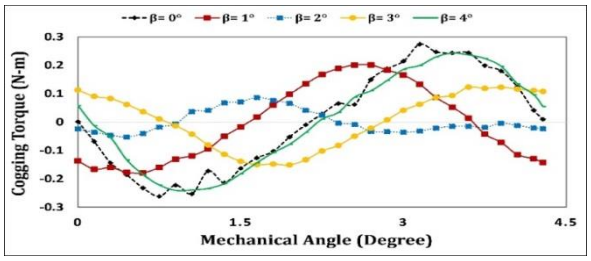

(b)

Fig. 5. Proposed PM segmentation (S=2), (a) The arrangement of rotor and PM segments, (b) Cogging torque waveforms

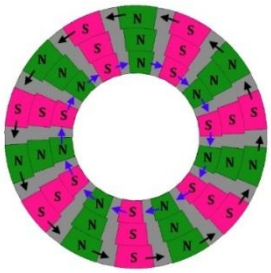

(a)

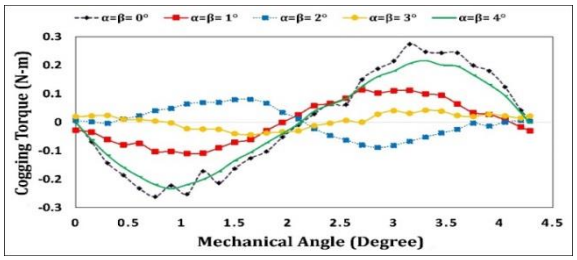

(b)

Fig. 6. Proposed PM segmentation (S=3), (a) The arrangement of rotor and PM segments, (b) Cogging torque waveforms

The radial length of the segments is equal. The middle PM segments are kept fixed, while the down PM segments are shifted clockwise with the α shift angle, and the up PM segments are shifted counter-clockwise with the β shift angle. As can be seen from Figure 6.b, by implementing several three-dimensional FEA, the cogging torque waveforms of the YASA-AFPM generator are estimated for the different shift angles from $= \beta = 0^{\circ}$ to $\alpha = \beta = 4^{\circ}$. The minimum peak-to-peak value of the cogging torque is calculated as about 0.0703 N.m (approximately 87% reduction comparing the reference machine) and happened for $\alpha = \beta = 1.5^{\circ}$. Because the proposed PM segmentation for (S=3) has significantly mitigated the cogging torque (about 87%), therefore, due to the increasing complexity of the model, there is no need to evaluate the effectiveness of this technique for more than 3 segments.

Regarding the above-mentioned results, regardless of how many segments each PM pole is divided into, the suggested technique is useful and very effective in mitigation of the cogging effect in AFPM machines. According to what follows, the effectiveness of this technique can be justified. By shifting the PM segments of each magnet pole relative to each other, the resultant cogging torque of each pole is equal to the sum of the phase-shifted shares of each PM segment. At each permanent magnet pole, the up and down PM segments can be shifted relative to each other in such a way that their contribution of cogging torque becomes out of phase; thus, the resultant cogging torque becomes smaller.

The greatest effect of cancellation on the cogging torque harmonics occurs for a given shift angle, which can be determined using several 3D FEA simulations. It should be mentioned that by shifting the up PM segments relative to the down ones, the distance between the neighbor poles is kept constant and, as a result, the leakage flux component of the PMs does not increase; therefore, it is expected that the air-gap mean flux density would not decrease in this technique.

4.4. The impacts of the studied techniques on the generator load-ability and cogging torque

In the column chart shown in Figure 7.a, the lowest peak-to-peak value of the cogging torque obtained for the reference machine (original model) is compared with those values obtained from the different investigated cogging reduction techniques. With a reduction of about 87%, the conventional PM skewing and the proposed PM segmentation with S = 3 are the most effective techniques in reducing the cogging torque. The proposed segmentation method with S = 2 leads to a reduction of about 74% in cogging torque. The conventional PM segmentation methods with S = 2 and S = 3 lead to a cogging torque reduction of about 49% and 39%, respectively.

Generally, the cogging torque mitigation techniques result in an adverse impact on the machine output power. Certainly, the technique that can provide more mitigation in the cogging torque and at the same time have a less adverse impact on the generator load-ability is a more appropriate technique. Thus, the impact of the investigated cogging reduction techniques on the generator output power should be studied, too. For this

purpose, using several 3D FEA simulations, the load-ability characteristics of the YASA-AFPM generator with different magnet arrangement are evaluated and shown in Figure 7.b. The load-ability characteristic of the investigated generator is confirmed via the experimental test results [27]. Figure 8 illustrates the used experimental setup.

As shown in Figure 7.b, the proposed PM segmentation method has a negligible adverse effect on the generator load-ability, especially for S=2. In addition, it can be observed that the conventional segmentation method leads to a further reduction in the generator load-ability compared to the proposed segmentation method. Although the conventional PM skewing approach results in about 87% reduction in the cogging torque, it results in a large reduction in the generator load-ability, too. Thus, the proposed segmentation method is a more appropriate method compared to the other investigated methods. For the rated load current (8 A), the output power reduction compared to the reference machine is obtained as about 1.2%, 4.26%, 10.06%, 12.16%, and 24.46%, respectively for the proposed segmentation (S=2), the proposed segmentation (S=3), the conventional segmentation (S=2), the conventional segmentation (S=3), and the conventional PM skewing. Implementing the 3D FEA, for the reference YASA-AFPM machine, the output power (at rated current) is determined as 1009.61 watts.

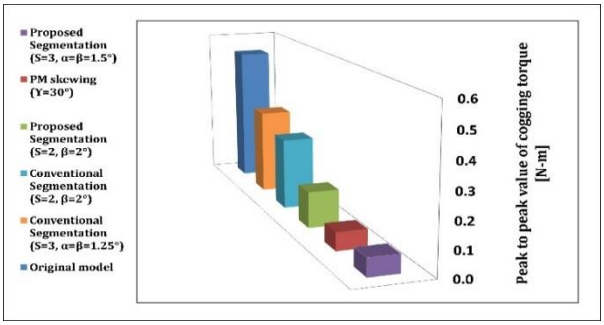

(a)

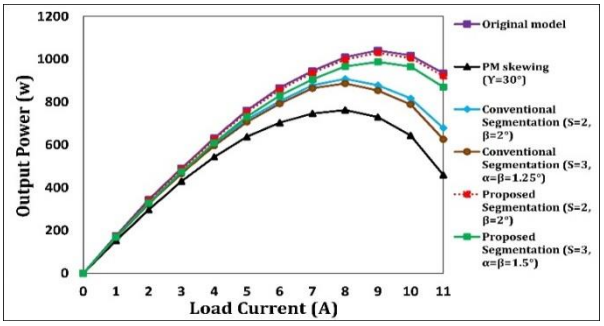

(b)

Fig. 7. Comparison of the cogging torque reduction methods, (a) Cogging torque values, (b) Generator load-ability

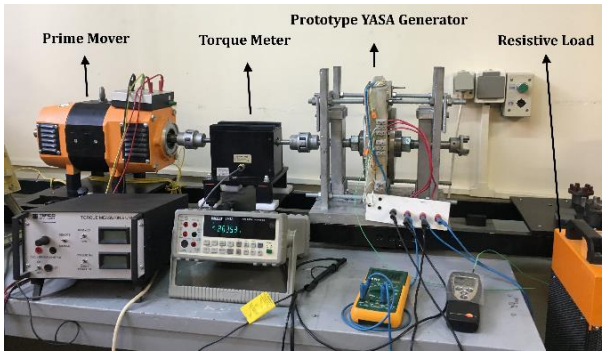

Fig. 8. The experimental setup [27]

Comparing the proposed PM segmentation technique for S=2 and S=3, based on their percentage of cogging torque mitigation and their adverse effect on the load-ability, it can be inferred that the PM segmentation for S=3 is of more effectiveness compared to the PM segmentation for S=2. For S=3, a considerable reduction of the cogging torque (about 87%) can be achieved and simultaneously, the load-ability can be maintained. As well, eddy current losses of the PMs can be further reduced. In the suggested technique, the shift angles for the up and down PM segments are considered equal. However, to achieve the most mitigation in the cogging torque and to preserve the generator load-ability, the values of shift angles should be optimized. In the next section, the optimal shift angles of the up and down PM segments are obtained using the design of experiments (DOE) approach.

5. OPTIMIZATION OF PM SEGMENTS SHIFT ANGLES USING DOE

In recent years, response surface methodology has been one of the most widely used methods for optimizing electrical machines. In Ref. [33], the RSM is applied to minimize cogging torque in the BLDC motors. In Ref. [34], torque maximization and magnetic field density optimization in the radial air gap of a permanent magnet spherical motor are performed using the Taguchi method, and the final optimization parameters are determined using the response surface method. In Ref. [35], the effect of the main design parameters on the performance of a reluctance synchronous machine is investigated, and an optimization method based on the response surface methodology along with the finite element model is used to maximize the torque density and efficiency of the machine. In Ref. [36], for a line-start PM motor, the design of the rotor shape was optimized by applying the RSM. In Ref. [37], the cogging torque of a hybrid axial and radial flux PM machine is optimized via applying the RSM and GA, and the validity of these techniques is verified via 3D FEA results. In Ref. [24], the cogging torque of an

AFPM machine with a soft magnetic composite core was minimized using the RSM and 3D FEA.

In this paper, an efficient approach is suggested for the cogging torque mitigation in the YASA-AFPM machines. The suggested technique is based on the segmentation of PMs into 2 or 3 segments in the radial direction and shifting the up and down PM segments in the circumferential direction with appropriate shift angles. The goal of this section is to specify the optimal shift angles aiming at minimizing the generator cogging torque and maintaining the generator load-ability. To this end, DOE is used in an optimal design process. DOE is a fast statistical technique to optimize the performance of systems with known input variables. The DOE begins with a screening experimental design test plan consisting of all the known factors that probably affect the system's performance (or output). If the number of input variables or experimental factors is large, the main experimental purpose is to decrease the input variables to a manageable number.

Once the screening experiment is done to find the main test factors, the next step is to conduct a response surface experiment [38]. A response surface method (RSM) is performed based on the selected design parameters and generated experimental data. The RSM is a set of beneficial statistical and mathematical techniques that are applied for analyzing and modeling problems in which the desired response is affected by several variables and the goal is optimizing this response. The RSM allows the exploration and optimization of response surfaces, where the response variable of interest is related to a set of input design variables [39]. Figure 9 shows the flowchart of the optimal design process using DOE, which can be roughly classified into two steps, including screening operation using the design of experiments to select the main design parameters and the optimal design process using the response surface methodology.

5.1. Screen activity to select main Factor

Several parameters can affect the cogging torque of the YASA-AFPM machines. If many parameters are defined as design variables, it takes large simulation time because of a large number of the required experiments. Therefore, to achieve better results, the number of design variables (factors) used in DOE should be reduced to a manageable few. Considering that by radially partitioning the PMs into three segments and shifting the up and down PM segments circumferentially with suitable shift angles, the generator cogging torque can be mitigated significantly, thus, in this study, the shift angles of the up and down PM segments (α, β) are considered as the design variables.

5.2. Optimization process using RSM

The response surface method is performed according to the selected design parameters. RSM searches for the relationship between an objective function and the design parameters in an interesting area through the statistical fitting method. The responses are generally obtained from real experiments or using computer simulations. In this paper, the 3D FEA technique is applied to analyze the YASA-AFPM machine and estimate the cogging torque and output power of the generator.

At first, a suitable statistical model for the response surface is considered, and the data are provided by performing experiments (3D FEA simulations) in various conditions of the independent variables. After that, a regression analysis is applied to estimate an approximation function [40]. As below relation, a polynomial approximation function is commonly utilized to construct the second-order fitted response surface:

$$y = \beta_0 + \sum_{j=1}^{2} \beta_j x_j + \sum_{i \neq j}^{2} \beta_{ij} x_i x_j + \sum_{j=1}^{2} \beta_{jj} x_j^2 + \varepsilon \quad (4)$$

Where y is the response variable; x_1 and x_2 are the design parameters; $\beta_0, \beta_j, \beta_{ij}, and\ \beta_{jj}$ are regression coefficients estimated by regression from experiments; and ε is the estimation error.

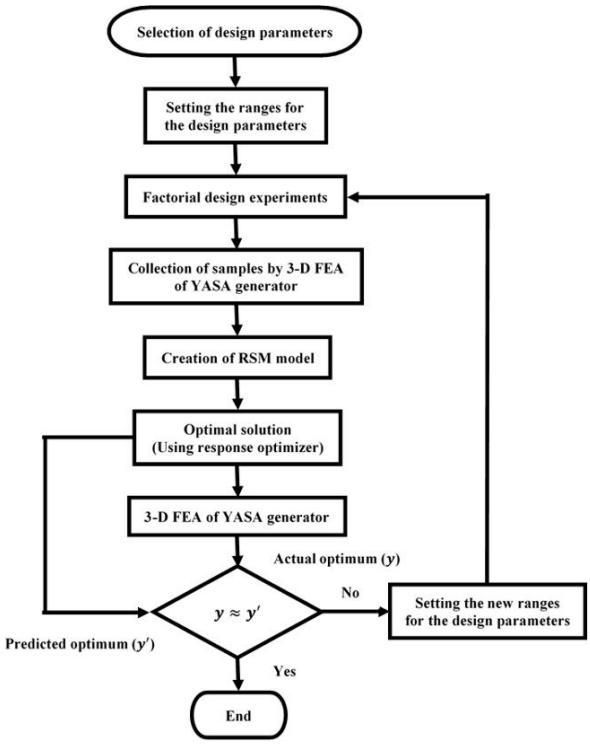

Fig. 9. Optimal design process using RSM

For obtaining the second-order fitted response surface, DOE must constitute at least 3 levels of any design variable. So, instead of the 3^k full factorial experiment scheme, the central composite design (CCD) is used for creating the second-order fitted model [41]. To determine the accuracy of the regression equation from the CCD, the coefficient of determination R^2 can be used as below:

$$R^2 = \frac{\text{SSR}}{\text{SST}} \tag{5}$$

Where SSR and SST are given as follows:

$$\text{SSR} = \sum_{u=1}^{N} \left(\hat{Y}_u - \bar{Y}\right)^2 \tag{6}$$

$$\text{SST} = \sum_{u=1}^{N} \left(Y_u - \bar{Y}\right)^2 \tag{7}$$

Where N is the number of total experiments in the CCD, Y is the actual response value, $\bar{Y}$ is the average response value, and $\hat{Y}$ is the response value from the regression equation.

In this paper, the second-order fitted model of F_{obj} is used as the objective function. To reduce the generator cogging torque and maintain the generator load-ability (output power), two objective functions are adopted. F_{obj1} is the cogging torque (peak-to-peak value) and F_{obj2} is the YASA-AFPM generator output power (at the rated current).

5.3. Analysis of the design results

It is shown that by radially dividing magnets into 3 segments and circumferentially shifting the up and down segments with appropriate shift angles, the cogging torque of the YASA-AFPM machine can be reduced effectively. To obtain the optimal shift angles, the shift angles of the up segments (α) and down segments (β), are considered as the design variables. As depicted in Figure 9, once the design variables being chosen, the variable space must be specified. To attain a low cogging torque and maintain the generator load-ability, the initial variable space is considered as ($1^\circ \leq \alpha \leq 4^\circ, 1^\circ \leq \beta \leq 4^\circ$). For the initial operation region, the main effects plot of the cogging torque and output power (at the rated current) are obtained and depicted in Figure 10. With the two design variables, the CCD must conduct 13 experiments. After taking the experimental data by 3D FEA, the function to plot the response surface is extracted. The goals of this study are minimizing the F_{obj1} and maintaining the F_{obj2} (F_{obj1} and F_{obj2} are specified until now).

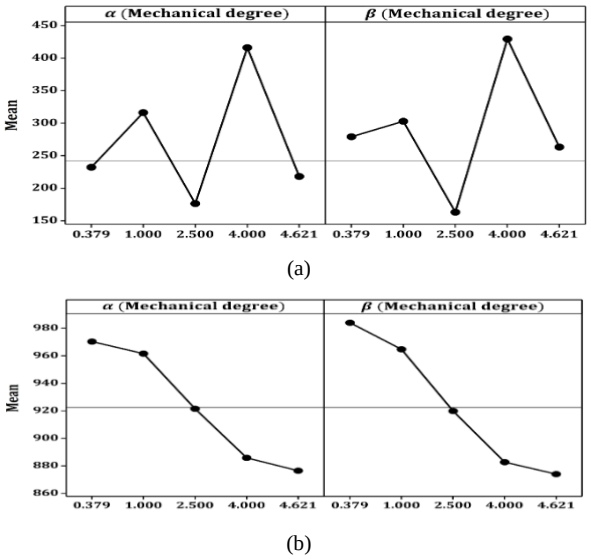

(a)

(b)

Fig. 10. Main effects plot for, (a) The cogging torque (mN-m), (b) The output power (watt)

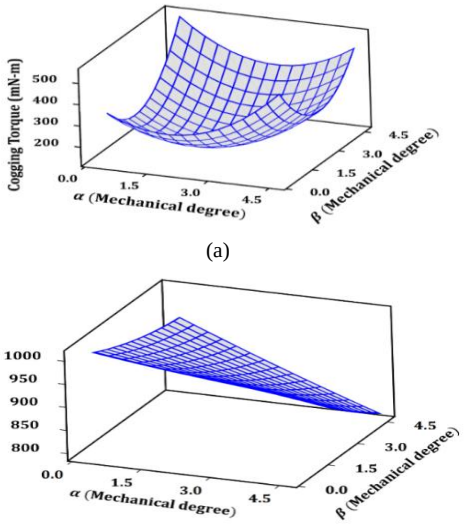

(a)

(b)

Fig. 11. The RSPs of the YASA-AFPM machine, (a) cogging torque (peak-to-peak), and (b) output power

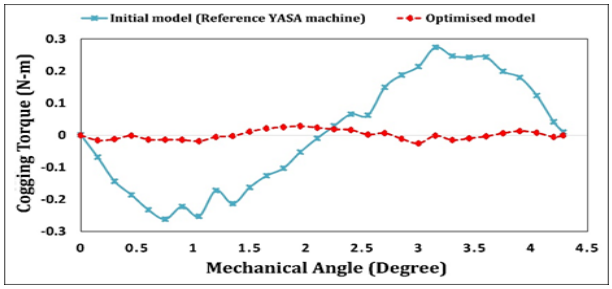

Fig. 12. Cogging torque of the original and optimal design (based on the RSM optimizer design)

For the initial operation region ($1^\circ \leq \alpha \leq 4^\circ, 1^\circ \leq \beta \leq 4^\circ$), the two fitted second-order polynomial of the objective functions for the two variables are:

$$F_{\text{obj1}} = 438.525 - 113.613\alpha - 160.62\beta + 32.3692\alpha^2 + 42.609\beta^2 - 13.297\alpha\beta \tag{8}$$

$$F_{\text{obj2}} = 1022.93 - 12.0514\alpha - 21.2113\beta + 0.81761\alpha^2 + 2.06034\beta^2 - 6.28624\alpha\beta \quad (9)$$

As mentioned earlier, the coefficient of determination R^2 is used to determine the accuracy of the regression equation from the CCD. The coefficient of determination R^2 for F_{obj1} is 0.7058 and indicates that 70.58% of the entire variation in the cogging torque can be explained via the regression equation. Also, R^2 for F_{obj2} is 0.9972 and indicates that 99.72% of the entire variation in the produced power of the YASA-AFPM machine can be explained via the regression equation. For the initial operation region ($1^\circ \le \alpha \le 4^\circ, 1^\circ \le \beta \le 4^\circ$), the response surface plots (RSPs) of cogging torque and output power are obtained and shown in Figure 11.

Based on the flowchart presented in Figure 9, to minimize cogging torque and preserve produced power of the investigated YASA machine, the optimization of shift angles is accomplished via DOE. The optimization results, which are obtained after several iterations using the Minitab software response optimizer, indicate that the optimum shift angles for the down and up PM segments are $\alpha = 1.4307^\circ$ and $\beta = 1.5532^\circ$, respectively. Also, based on the response optimizer results, for the optimum shift angles, the peak-to-peak value of cogging torque is predicted as 0.054 N-m, and the YASA-AFPM generator output power (for the nominal load current) is predicted as 979.51 watts. For the optimal shift angles obtained using the response optimizer, the 3D model of the YASA-AFPM generator is created in the Maxwell software, and the corresponding cogging torque waveform is obtained using 3D FEA, as shown in Figure 12. As specified by the figure, the estimated peak-to-peak value of the cogging torque for the optimal YASA-AFPM generator is 0.0542 N-m, shows a reduction of approximately 90% compared with the reference generator. Also, the optimal output power of the YASA-AFPM generator (for the rated load current), estimated via the 3D FEA, is 976.48 watts, which shows a reduction of about 3.28% compared to the reference case. The values of the cogging torque and output power of the YASA-AFPM generator, calculated from three-dimensional FEA, are in good agreement with those estimated from the response optimizer.

6. CONCLUSIONS

An effective cogging torque mitigation method for the AFPM machines with a yokeless and segmented armature was investigated in this paper. The suggested technique is based on the segmentation of PMs into a few segments in the radial direction and shifting some of the PM segments in the circumferential direction with suitable shift angles. Compared with a number of the cogging torque reduction methods presented in the literature, such as double, triangular, or trapezoidal PM skewing, using two-layer magnets, using multiple rectangular magnets at each pole, and applying combined methods, the suggested approach is less complex. In addition, comparing the proposed method with the conventional PM segmentation and the conventional PM skewing methods, it was observed that the proposed method is more effective in reducing the cogging torque and has a less negative effect on the generator load-ability. The efficacy of the number and shift angles of the PM segments on the produced power and cogging torque value of the YASA-AFPM machine was examined via 3D FEA. Regardless of the number of PM segments, the suggested technique is very effective in cogging torque mitigation of the YASA-AFPM machines; however, the division of magnets into three segments instead of two segments results in a greater cogging reduction. Using DOE and RSM, the optimal shift angles of the PM segments were obtained to reduce the cogging torque and maintain the YASA-AFPM generator load-ability. The optimal shift angles were verified by 3D FEM. It was shown that, for the optimal shifting angles of $\alpha = 1.4307^\circ$ and $\beta = 1.5532^\circ$, respectively for the down and up PM segments, compared to the reference YASA-AFPM machine (initial model), the cogging torque can be reduced about 90%, while the output power (at the nominal load) decreases only 3.28%.

REFERENCES

[1] J. Kim, W. Choi and B. Sarlioglu, "Closed-form solution for axial flux permanent-magnet machines with a traction application study", *IEEE Trans. Ind. Appl.*, vol. 52, pp. 1775-84, 2016.

[2] Z. Zhang, W. Geng, Y. Liu and C. Wang, "Feasibility of a new ironless-stator axial flux permanent magnet machine for aircraft electric propulsion application", *CES Trans. Electr. Mach. Syst.*, vol. 3, pp. 30-38, 2019.

[3] N. Anitha and R. Bharanikumar, "Design and analysis of axial flux permanent magnet machine for wind power applications", Proc. *PETPES*, Mangalore, India, 2019.

[4] P. Ojaghlu and A. Vahedi, "Specification and design of ring winding axial flux motor for rim-driven thruster of ship electric propulsion", *IEEE Trans. Veh. Technol.*, vol. 68, pp. 1318-26, 2019.

[5] T. Woolmer and M. McCulloch, "Analysis of the yokeless and segmented armature machine", Proc. *IEMDC*, Antalya, Turkey, 2007.

[6] L. Xu et al., "Optimal design and electromagnetic analysis of yokeless and segmented armature machine based on finite-element method and genetic algorithm", Proc. *ITEC Asia-Pacific*, Harbin, China, 2017.

[7] A. EL-Refaie, "Fractional-slot concentrated-windings

synchronous permanent magnet machines: opportunities and challenges", *IEEE Trans. Ind. Electron.,* vol. 57, pp. 107-121, 2010.

[8] B. Rocandio, "Design and analysis of fractional-slot concentrated-winding multiphase fault-tolerant permanent magnet synchronous machines", Ph.D. dissertation, University of Navarra, Pamplona, Spain, 2015.

[9] J. Ji, H. Chen and W. Zhao, "Reduction of eddy current loss of permanent-magnet machineswith fractional slot concentrated windings", *Prog. Electromagn. Res. Lett.,* vol. 56, pp. 39-46, 2015.

[10] T. Gundogdu and G. Komurgoz, "Investigation of winding MMF harmonic reduction methods in IPM machines equipped with FSCWs", *Int. Trans. Electr. Energy Syst.,* pp. 1-27, 2018.

[11] J. Li, R. Qu, Y. Cho and D. Li, "Reduction of eddy-current losses by circumferential and radial PM segmentation in axial flux permanent magnet machines with fractional-slot concentrated winding", *Proc. INTERMAG*, Beijing, China, 2015.

[12] J. Li et al., "Minimization of cogging torque in fractional-slot axial flux permanent magnet synchronous machine with conventional structure", Proc. I*CEF*, Dalian, Liaoning, China, 2012.

[13] S. Ho, S. Niu and W. Fu, "Design and comparison of vernier permanent magnet machines", *IEEE Trans. Magn.,* vol. 47, pp. 3280-83, 2011.

[14] A. Kumari, S. Marwaha and A. Marwaha, "Comparison of methods of minimization of cogging torque in wind generators using FE analysis", *J. Indian Inst. Sci.,* vol. 86, pp. 355-362, 2006.

[15] M. Gulec and M. Aydin, "Magnet asymmetry in reduction of cogging torque for integer slot axial flux permanent magnet motors", *IET Electr. Power Appl.,* vol. 8, pp. 189-198, 2014.

[16] L. Jia et al., "Dual-skew magnet for cogging torque minimization of axial flux PMSM with segmented stator", *IEEE Trans. Magn.,* vol. 56, 2020.

[17] J. Gao et al., "Cogging torque reduction by elementary-cogging-unit shift for permanent magnet machines", *IEEE Trans. Magn.,* vol. 53, pp. 1-4, 2017.

[18] E. Aycicek, N. Bekiroglu and S. Ozcira, "An experimental analysis on cogging torque of axial flux permanent magnet synchronous machine", *Proc. Natl. Acad. Sci., India, Sect. A Phys. Sci.,* vol. 86, pp. 95-101, 2016.

[19] L. Xiao et al., "Cogging torque analysis and minimization of axial flux PM machines with combined rectangle-shaped magnet", *IEEE Trans. Ind. Appl.,* vol. 53, pp. 1018-1027, 2017.

[20] P. Kumar, M. Reza and R. Srivastava, "Effect of cogging torque minimization techniques on performance of an axial flux permanent magnet machine", *Proc. ITEC-India*, Pune, India, 2017.

[21] M. Aydin and M. Gulec, "Reduction of cogging torque in double-rotor axial-flux permanent-magnet disk motors: a review of cost-effective magnet-skewing techniques with experimental verification", *IEEE Trans. Ind. Electron.,* vol. 61, pp. 5025-34, 2014.

[22] O. Ocak and M. Aydin, "A new variable step skew approach for minimizing torque pulsations in permanent magnet synchronous motors", *Proc. INTERMAG*, Singapore, 2018.

[23] J. Kim, Y. Li, E. Cetin and B. Sarlioglu, "Influence of rotor tooth shaping on cogging torque of axial flux-switching permanent magnet machine", *IEEE Trans. Ind. Appl.,* vol. 55, pp. 1290-98, 2019.

[24] L. Xu, Y. Xu and J. Gong, "Analysis and optimization of cogging torque in yokeless and segmented armature axial-flux permanent-magnet machine with soft magnetic composite core", *IEEE Trans. Magn.,* vol. 54, pp. 1-5, 2018.

[25] A. Patel and B. Suthar, "Double layer magnet design technique for cogging torque reduction of dual rotor single stator axial flux brushless DC motor", *Iran J. Electr. Electron. Eng.,* vol. 16, pp. 58-65, 2020.

[26] Y. Wang et al., "Reduction of magnet eddy current loss in PMSM by using partial magnet segment method", *IEEE Trans. Magn.,* vol. 55, pp. 1-5, 2019.

[27] S. Arand and M. Ardebili, "Multi-objective design and prototyping of a low cogging torque axial-flux PM generator with segmented stator for small-scale direct-drive wind turbines", *IET Electr. Power Appl.,* vol. 10, pp. 889-899, 2016.

[28] D. Hanselman, Brushless permanent magnet motor design, Ohio: Magna Physics Publishing, 2006.

[29] T. Li and G. Slemon, "Reduction of cogging torque in PM motors", *IEEE Trans. Magn.,* vol. 24, pp. 2901-03, 1988.

[30] N. Rostami, "Comprehensive parametric study for design improvement of a low-speed AFPMSG for small scale wind-turbine", *J. Oper. Autom. Power Eng.,* vol. 7, pp. 58-64, 2019.

[31] D. Habibinia, M. Feyzi and N. Rostami , "A new method for computation of axial flux permanent magnet synchronous machine inductances under saturated condition", *J. Oper. Autom. Power Eng.,* vol. 6, pp. 208-217, 2018.

[32] D. Gonzalez, J. Tapia and A. Bettancourt, "Design consideration to reduce cogging torque in axial flux permanent-magnet machines", *IEEE Trans. Magn.,* vol. 43, pp. 3435-40, 2007.

[33] S. Arslan, E. Kurt, O. Akizu and J. Lopez-guede, "Design optimization study of a torus type axial flux machine", *J. Energy Syst.,* vol. 2, pp. 43-56, 2018.

[34] J. He et al., "Optimization of permanent-magnet spherical motor based on taguchi method", *IEEE Trans. Magn.,* vol. 56, pp. 1-7, 2020.

[35] H. Moghaddam, A. Vahedi and S. Ebrahimi, "Design optimization of transversely laminated synchronous reluctance machine for flywheel energy storage system using response surface methodology", *IEEE Trans. Ind. Electron.,* vol. 64, pp. 9748-57, 2017.

[36] S. Saha, G. Choi and Y. Cho, "Optimal rotor shape design of LSPM with efficiency and power factor improvement using response surface methodology", *IEEE Trans. Magn.,* vol. 51, pp. 1-4, 2015.

[37] S. Sun, F. Jiang, T. Li and K. Yang, "Optimization of cogging torque in a hybrid axial and radial flux permanent magnet machine", *Proc. ICEMS*, Harbin, China, 2019.

[38] M. Uy and J. Telford, "Optimization by design of experiment techniques", *Proc. IEEE Aero Conf.*, Big Sky, MT, 2009.

[39] D. Montgomery, Design and Analysis of Experiments: Response surface method and designs, New Jersey: John Wiley and Sons, 2005.

[40] A. Khyri and J. Cornell, Response Surfaces: Designs and Analyses, New York: Marcel Dekker, 1996.

[41] B. Khuri, Response Surface Methodology and Related Topics, New Jersey: World Scientific Pub Co Inc, 2006.